Molecular Counting with Localization Microscopy: A Redundant Labeling Approach

Daniel Nino,[1,2] Yong Wang,[3] Anton Zilman,[1] and Joshua N. Milstein[1,2,*]

[1]*Department of Physics, University of Toronto, Toronto, ON CAN*

[2]*Department of Chemical and Physical Sciences, University of Toronto Mississauga, Mississauga, ON CAN*

[3]*Department of Physics, University of Arkansas, Fayetteville, AR USA*

(Dated: August 23, 2016)

Abstract

Super-resolved localization microscopy (SLM) has the potential to serve as an accurate, single-cell technique for counting the abundance of intracellular molecules. However, the stochastic blinking of single fluorophores can introduce large uncertainties into the final count. Here we provide a theoretical foundation for applying SLM to the problem of molecular counting in such a way as to mitigate errors introduced by stochastic blinking. We show that by redundantly tagging single-molecules with multiple blinking fluorophores, the accuracy of the technique can be enhanced by harnessing the central limit theorem. The coefficient of variation (CV) then, for the number of molecules M estimated from a given number of blinks B, scales like $\sim 1/\sqrt{N_l}$, where N_l is the mean number of labels on a target. As an example, we apply our theory to the challenging problem of quantifying the cell-to-cell variability of plasmid copy number in bacteria.

* Corresponding Author: josh.milstein@utoronto.ca

I. INTRODUCTION

Cell biology is becoming increasingly quantitative with advances in light microscopy strongly driving this trend. Beyond imaging structure, significant effort has been put into developing microscopy based approaches to determining the abundance of proteins and nucleic acids in cells [1, 2]. Molecular counting experiments can provide insight into cellular structure and define the stoichiometry of interacting protein complexes. Moreover, since microscopy provides information at the single-cell level, it may be used to study stochastic variation within a population due to varying levels of mRNA and protein copy number, which is inaccessible to bulk techniques [3]. This variability is thought to be a crucial component of many biological processes such as cellular differentiation and evolutionary adaptation [4, 5].

A fluorescence based approach to molecular counting would be particularly powerful in single-cell 'omics' applications where a low level, such as trace amounts of protein, DNA, or RNA, must be detected [6, 7]. A reduction or even elimination of the amplification stage prior to sequencing of DNA or RNA could greatly increase the accuracy and reliability of single-cell genomic analyses. And since fluorescence microscopy is less susceptible to errors arising from protein size or abundance than techniques like mass spectroscopy [8], it could hold a significant advantage for single-cell proteomics.

Most conventional microscopy techniques either rely upon observing the step-wise photobleaching of fluorescent labels or on calibrating the fluorescence intensity to a standard [1, 2, 9]. While these two methods have provided valuable insight into a range of cellular phenomena, both have their limitations. Step-wise photobleaching can only be used to identify small numbers of molecules (roughly < 10). And intensity measurements, although able to quantify the number of more abundant molecules, are hindered by stochastic variation in photon emission, photodepletion and collection efficiency, and are limited by the dynamic range of the detection camera. Likewise, both techniques have difficulties when observing diffraction limited fine structures due to overlapping signal from neighbouring features.

Super-resolved localization microscopy (SLM), which include techniques such as PALM [10] and dSTORM [11], could provide an alternative approach that would not suffer from these limitations. SLM can produce images of structural detail an order-of-magnitude finer than diffraction limited techniques. The method relies on precisely localizing the spatial position of single, fluorescent labels attached to an assembly of target molecules. This typically

requires the use of photo-convertible or photo-activatable fluorophores that can be induced to blink in such a way that only a random subset of the labels are visible during each frame [12, 13]. For a sufficiently sparse image, each diffraction limited spot should be sufficiently well separated, and the subset of fluorophores may be localized with a precision that scales like $\sim 1/\sqrt{P}$, where P is the mean number of photons collected from a single blink of a fluorophore. Tens of thousands of frames are typically acquired, the spatial coordinates of the fluorophores within each frame extracted, and the resulting data from the stack rendered into a final image.

Since SLM measures discrete blinks from single fluorescent labels, it essentially provides a digital approach to molecular counting, compared to conventional techniques that measure the overall amplitude of a signal, and are akin to an analog method [14–16]. However, there are several challenges to obtaining accurate counts with SLM, most notably, accounting for multiple blinks from a single fluorophore and the inefficiency with which the fluorophores photo-activate or photo-convert [17, 18]. Both issues lead to an inaccuracy in estimating the total number of molecules [15, 16, 19], and there has been much effort to mitigate these difficulties [14, 16, 20–25].

In this manuscript, we lay out a mathematical foundation for estimating molecular number and the accuracy of such estimates from SLM data. While the stochastic blinking of the fluorophores can introduce uncertainty when translating between the number of localizations and the number of molecules, we show how this uncertainty can be reduced by labeling single molecules with multiple labels. As an example, we apply our theory to design an experiment that measures the cell-to-cell variability of plasmid copy number in bacteria (a task that has proven to be surprisingly difficult [26]).

II. RESULTS

A. Counting single molecules from blinking fluorophores

Let's begin by calculating the conditional probability distribution $P(B|N)$ for observing B blinks (or localizations) from a set of N fluorophores during a measurement time T_M. We assume the only information available is the total number of blinks B, and ignore any spatial information contained within the data that might enable us to differentiate one fluorophore

from another. In the simple case of a single emitter, the probability $P(B|N)$ is often well satisfied by a geometric distribution [16]:

$$P(B|N=1) = (1 - e^{-1/\lambda})e^{-B/\lambda}, \tag{1}$$

where λ is the characteristic number of blinks of a particular fluorophore within the interval T_M. From this relationship we generalize to the case of N fluorophores to obtain the distribution

$$P(B|N) = \binom{B+N-1}{N-1}\left(1 - e^{-1/\lambda}\right)^N e^{-B/\lambda}, \tag{2}$$

where the prefactor accounts for the number of ways that N fluorophores, each blinking some B_i times, can yield $\sum_{i=1}^{N} B_i = B$ blinks. The mean and variance of Eq. 2 (see Appendix A) are:

$$\mu_B = \frac{N}{(e^{1/\lambda} - 1)}, \tag{3}$$

and

$$\sigma_B^2 = \frac{\mu_B^2}{N} e^{1/\lambda}, \tag{4}$$

respectively.

Up until this point, we have been considering the conditional probability distribution $P(B|N)$, which, to reiterate, is the probability of observing B blinks when there are N fluorophores. However, we wish to know the probability of there being N fluorophores when we observe B blinks, or $P(N|B)$. Bayes' Theorem connects these two expressions

$$P(N|B) = \frac{P(B|N)P(N)}{P(B)}. \tag{5}$$

If we have no prior knowledge of the distribution of fluorophores in our sample we may set $P(N)$ as a constant. This yields the maximum likelihood (ML) approximation to the posterior distribution $P(N|B)$. The two distributions are then proportional $P(N|B) \propto P(B|N)$.

It is customary to define a log likelihood function $\mathcal{L}(N, B) = -\ln P(N|B)$. For a sharply peaked, symmetric distribution, the maximum with respect to N (i.e., $\partial\mathcal{L}(N, B)/\partial N|_{\mu_N} = 0$) should roughly correspond to the mean number of molecules:

$$\mu_N = B(e^{1/\lambda} - 1). \tag{6}$$

Likewise, we can obtain the variance in the estimated number of molecules, which provides the accuracy of the estimate, by rewriting the conditional probability and Taylor expanding as follows:

$$P(N|B) = e^{-\mathcal{L}(N,B)} \propto e^{-\frac{1}{2}\frac{\partial^2 \mathcal{L}}{\partial N^2}\Big|_{\mu_N}(N-\mu_N)^2}. \tag{7}$$

In the exponent of Eq. 7, we identify the variance σ_N^2 from $\sigma_N^{-2} = \partial^2\mathcal{L}(N,B)/\partial N^2|_{\mu_N}$ to yield

$$\sigma_N^2 = \frac{\mu_N^2}{B}\frac{e^{1/\lambda}}{e^{1/\lambda}-1}. \tag{8}$$

For single fluorophores that blink multiple times during the measurement (i.e., the limit $\lambda \gg 1$), Eq. 6 simply reduces to the intuitive expression $\mu_N = B/\lambda$, which states that the most likely number of fluorophores is equal to the measured number of blinks divided by the mean number of blinks per fluorophore. In this limit, Eqs. 6 and 8 yield a Poisson distribution with $\sigma_N^2 = \mu_N$, and the coefficient of variation (CV), which quantifies the variability of the estimate relative to the mean ($\eta \equiv \sigma_N/\mu_N$), is simply $\eta = 1/\sqrt{\mu_N}$.

B. Accounting for multiple labels on a target

There are a myriad of labeling techniques in cell biology and the correspondence between the number of fluorophores and the number of target molecules is typically not one to one. For instance, immunolabeled molecules will contain several dyes on each antibody and covalently labeled proteins will often be tagged at multiple residues. The probability of having N fluorophore labels in total when there are M target molecules, each with h possible sites where a fluorophore may bind (or hybridize), is given by the binomial distribution

$$P(N|M) = \binom{hM}{N}\theta^N(1-\theta)^{hM-N}, \tag{9}$$

where θ denotes the fractional occupancy. Note that hM is the maximum number of labels possible, if we ignore all non-specific labeling, and that the fractional occupancy θ ranges from $0 \leq \theta \leq 1$.

C. Distribution of blinks within a population

We can now combine Eqs. 2 and 9 as follows:

$$P(B|M) = \sum_N P(B|N)P(N|M), \tag{10}$$

to derive the conditional probability distribution for observing B blinks from a population of M fluorescently labeled molecules. While the full sum is quite cumbersome, although straightforward to evaluate numerically, the moments of Eq. 10 are analytically tractable. For instance, the first and second moments may be found by multiplying both sides of Eq. 10 by $\sum_B B$ or $\sum_B B^2$, respectively, and evaluating the summations. The first moment is the mean number of blinks

$$\tilde{\mu}_B = \frac{M\theta h}{e^{1/\lambda} - 1}, \tag{11}$$

which can be combined with the second moment to obtain the variance

$$\tilde{\sigma}_B^2 = \frac{\tilde{\mu}_B^2}{M\theta h}\left(e^{1/\lambda} + 1 - \theta\right). \tag{12}$$

However, we wish to estimate the mean and variance in the estimate of the number of molecules after having measured B blinks. While a more formal derivation is provided in Appendix B, the ML estimate for the mean can simply be obtained by substituting $\tilde{\mu}_B \to B$ and $M \to \tilde{\mu}_M$ into Eq. 11:

$$\tilde{\mu}_M = \frac{B(e^{1/\lambda} - 1)}{\theta h}. \tag{13}$$

In the limit $\lambda \gg 1$, Eq. 13 again yields an intuitive result for the expected number of molecules $\tilde{\mu}_M = B/(\lambda\theta h)$.

The variance, on the other hand, is more challenging to evaluate, but it can be estimated, similar to how one estimates the propagation of errors in a measurement (see Appendix C). If we assume the distribution $P(M|B)$ is peaked about the mean $\tilde{\mu}_M$, then we may use the following expression for the Fisher information matrix [27]:

$$\tilde{\sigma}_M^2 = \left(\frac{\partial\tilde{\mu}_M}{\partial B}\right)^2 \tilde{\sigma}_B^2, \tag{14}$$

to yield our final result for the ML estimate of the variance

$$\tilde{\sigma}_M^2 = \frac{\tilde{\mu}_M^2}{B}\frac{(e^{1/\lambda} + 1 - \theta)}{e^{1/\lambda} - 1}. \tag{15}$$

In the limit $\lambda \gg 1$, this yields the simpler expression $\sigma_M^2 = \tilde{\mu}_M^2(2-\theta)\lambda/B$, and the CV for this process is simply

$$\tilde{\eta}^2 = \frac{1}{\tilde{\mu}_M}\frac{(2-\theta)}{\theta h}, \tag{16}$$

which can, when $\theta h > 2 - \theta$, reach the sub-Poissonian limit scaling like one over the square root of the mean number of labels per molecule $\tilde{\eta} \propto 1/\sqrt{N_l}$, where $N_l \equiv \theta h$. This scaling, of course, is simply a result of the central limit theorem.

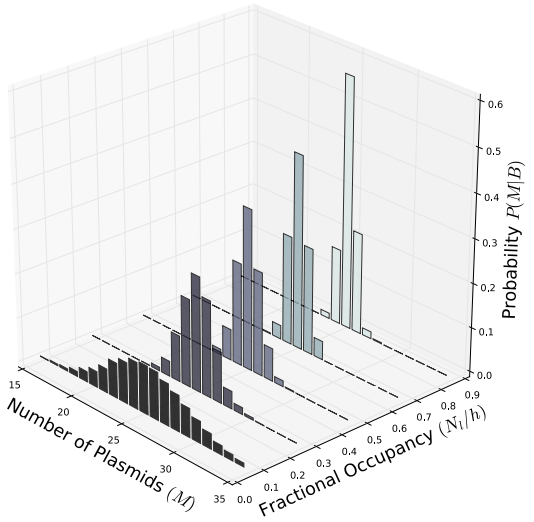

FIG. 1. The simulated probability distribution $P(M|B)$ for ($M = 25$, $\lambda = 2$, $h = 96$) at fractional occupancies ($N_l/h = 0.05, 0.25, 0.45, 0.65, 0.85$) showing a sharper distribution (i.e., less uncertainty) at increasing occupancy.

III. CELL-TO-CELL VARIABILITY OF PLASMID COPY NUMBER

To illustrate the utility of our approach, we consider the problem of counting plasmids in single bacterial cells. Plasmids are circular, extra-chromosomal segments of DNA that often confer a selective advantage, such as a resistance to antibiotics, to their host. Plasmids are also a relatively simple way to introduce genes into a cell making them an invaluable tool throughout molecular and synthetic biology. An important feature of a plasmid is its copy number. If a plasmid is harbouring a gene one wishes to express at a controlled level, variations in plasmid number will likely lead to varying levels of expression. While bulk techniques such as qPCR can place bounds on the average plasmid copy number, it has proven extremely difficult to quantify the copy number distribution within a population [26].

Localization microscopy could provide a way to measure the cell-to-cell variability in copy number. Super resolved localization microscopy images of a high-copy number ColE1 plasmid were recently obtained in fixed E. coli bacteria [28]. Atto-532 labeled DNA probes were annealed via DNA fluorescence in situ hybridization (FISH) to an array of LacO sites (256 sites) introduced in the target plasmids, then imaged by dSTORM. Furthermore, both the mean number of blinks λ and the fractional occupancy θ could be obtained from *in vitro*

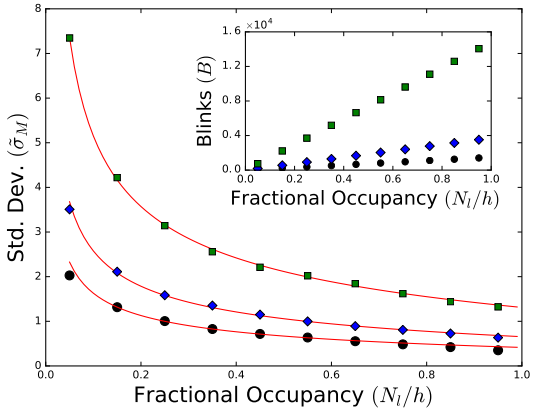

FIG. 2. Uncertainty in the number of molecules vs. fractional occupancy for $M = 10$ (circles) , 25 (diamonds), and 100 (squares), $\lambda = 2$ and $h = 96$. Solid lines are a theoretical estimate from Eq. 15. The insert shows the increase in the expected number of observed blinks, for these parameters, with increasing fractional occupancy.

measurements (from photoactivation of sparse samples of the dye and from photobleaching experiments on the hybridization of the probes to an array of the target sequence, respectively).

Here we consider targeting a 96 site array (a 96-TetO array, for instance, is commonly available [29]) to lessen the effects of the insert on the replication dynamics of the plasmid [30]. Figure 1 shows the probability distribution $P(M|B)$ for this hypothetical system. We've chosen $M = 25$ for illustrative purposes, but the qualitative results remain similar for different plasmid number (i.e., for increasing fractional occupancies, $N_l/h = \theta$, the distribution becomes increasingly peaked around the expected value). Figure 2 shows that as more blinks are observed, due to an increased fractional occupancy, for the same number of plasmids ($M = 10, 25, 100$), the error in the estimate of M rapidly decreases. As more probes associate with the plasmids, the coefficient of variation decreases like $\sim 1/\sqrt{N_l}$, and can be made to drop well below the Poisson limit $1/\sqrt{M}$ (see Fig. 3). This is illustrated for a range of plasmid number (again, $M = 10, 25, 100$). For $M = 25$, for instance, and a reasonable fractional occupancy as might be achieved by DNA FISH, say 20%, the error in a single-cell count would be only $\pm$1-2 plasmids. Unfortunately, the efficiency at which the probes hybridize in DNA FISH experiments is always hampered by the competing complementary DNA. Perhaps by employing peptide nucleic acid (PNA) probes [31], devoid of

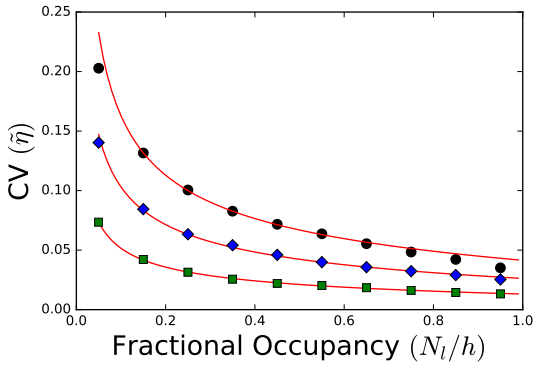

FIG. 3. Coefficient of variation ($\tilde{\eta}$) vs. fractional occupancy (N_l/h) for different plasmid (molecule) number: $M = 10$ (circles), 25 (diamonds), 100 (squares) ($\lambda = 2$ and $h = 96$). The solid lines are the theoretical estimate from Eq. 16. At, roughly, $M = 10$ the theory begins to deviate from the simulated results.

the negative charge along their backbone, the fractional occupancy could be enhanced to further reduce the uncertainty.

IV. DISCUSSION

The redundant labeling approach we present in this manuscript makes use of the central-limit theorem to improve on the accuracy of a molecular count, achieving a $\sqrt{N_l}$ improvement in the uncertainty of the estimated count (where N_l is the mean number of labels per molecule). Our approach relies upon an accurate measure of two parameters: the mean number of blinks from a single fluorophore λ during the measurement time and the fractional occupancy θ. Let's assume that *in vitro* measures of these parameters are accurate. The parameter λ can easily be obtained from imaging single blinking fluorophores sparsely attached to a coverslip. Obtaining the fractional occupancy, however, is more challenging. One method is to count photobleaching steps of single labeled probes bound to a target. In our plasmid example, the actual 96-TetO repeat target is much too large for such an approach, but it's reasonable to assume that a smaller (say, 10-15 repeat target) would extrapolate. While this would provide the full distribution of occupancy, a simpler strategy is to measure the resulting ratio of plasmid DNA to fluorophore labels (by absorption spectroscopy and fluorometry, respectively). The fractional occupancy can then be backed out of the underlying binomial distribution.

However, as mentioned, many fluorophores do not efficiently photo-activate or -convert. One might be be able to account for this aspect of the photophysics by quantifying the fractional occupancy using DNA origami [32]. For instance, in our plasmid example, an array of TetO sequences that could be spatially resolved by localization microscopy (e.g., patterned on a grid) would serve as a template. Inefficient photo-activation or -switching will simply lead to a reduced, measure of the fractional occupancy. Given a sufficient number of hybridization sites h, this should account for any underestimation in the molecular number due to inefficient photoswitching. In fact, an added advantage of labeling the actual plasmids with multiple labels is that the redundancy increases the odds that a signal will be received from each molecule. Finally, the reliability of *in vitro* measurements of the theoretical parameters could be tested. For instance, the fractional occupation could alternatively be measured *in vivo* by working with a low copy plasmid that could be spatially resolved via conventional microscopy, then performing a photobleach experiment to determine the number of probes hybridized to a single plasmid.

A redundant labeling approach is well adapted for counting plasmids because standard techniques for detecting specific DNA sequences, such as DNA FISH, require labeling with many fluorophore conjugated probes. However, the example is rather specialized, and it's often not feasible to attach multiple fluorophores to a single-molecule, such as when directly expressing fluorescently tagged proteins. On the other hand, standard immunolabeling techniques regularly target proteins with multiply labeled, fluorescently conjugated antibodies in order to achieve good signal intensity. Redundant labeling would reduce the uncertainty in quantifying the number of molecular components within diffraction limited clusters or aggregates via this commonly employed imaging technique.

Appendix A: Negative binomial distribution

Identifying Eq. 2 as a negative binomial distribution, the mean and variance can easily be derived from the moment generating function:

$$\Gamma(t) = \frac{(pe^t)^N}{[1-(1-p)e^t]^N}, \tag{A1}$$

where t is a dummy variable and, for consistency with Eq. 2, $p = 1-e^{-1/\lambda}$. The k^{th} moment is solved for by evaluating $\partial^k\Gamma(t)/\partial t^k\Big|_{t\to 0}$. From the first two moments, we once again obtain

Eqs. 3 and 4 for the mean and variance, respectively.

Appendix B: Derivation of the mean number of plasmids

To derive equation 13, we begin by expressing $P(M|B)$ analogous to Eq. 10 as

$$P(M|B) = \sum_N P(M|N)P(N|B). \tag{B1}$$

To calculate the mean, we can multiply both sides by $\sum_M M$ such that

$$\tilde{\mu}_M = \sum_N \left(\sum_M MP(M|N) \right) P(N|B) \tag{B2}$$

We approximate the term in brackets with the ML estimate of the expectation value of $P(M|N)$, which is $N/(\theta h)$. This leaves

$$\tilde{\mu}_M = \frac{1}{\theta h} \sum_N NP(N|B), \tag{B3}$$

where the remaining sum is identified as μ_N. Substituting the expression we derived in Eq. 6 yields Eq. 13.

Appendix C: Accuracy of ML estimate

If we Taylor expand the log likelihood function $\mathcal{L}(M, B) = -\ln P(M|B)$, assuming the distribution to be peaked about $\tilde{\mu}_B$, we can relate the likelihood function to the variance in the measured number of blinks:

$$\tilde{\sigma}_B^{-2} = \partial^2 \mathcal{L}(M, B)/\partial B^2 \Big|_{\tilde{\mu}_B}. \tag{C1}$$

However, we are interested in calculating the variance in the number of molecules $\tilde{\sigma}_M^2$, so let's assume that the probability distribution $P(M|B)$ is also peaked about $\tilde{\mu}_M$, and approximate its functional dependence as a Gaussian centred at $\tilde{\mu}_M$ with variance $\tilde{\sigma}_M^2$ [27]. In this case, the log likelihood function may be expressed as follows:

$$\mathcal{L}(M, B) = -\frac{(M - \tilde{\mu}_M)^2}{2\tilde{\sigma}_M^2} - \frac{1}{2} \ln \tilde{\sigma}_M^2. \tag{C2}$$

Since $\tilde{\mu}_M$ and $\tilde{\sigma}_M^2$ are both functions of B, we can evaluate the second derivative of Eq. C2 to obtain:

$$\frac{\partial^2 \mathcal{L}(p, B)}{\partial B^2}\Big|_{\tilde{\mu}_B} \approx \left(\frac{\partial \tilde{\mu}_M(B)}{\partial B} \right)^2 \Big|_{\tilde{\mu}_B} / \, \tilde{\sigma}_M^2(B)\Big|_{\tilde{\mu}_B}. \tag{C3}$$

Combining this result with Eq. C1 and solving for $\tilde{\sigma}_M^2$ yields Eq. 14.

ACKNOWLEDGMENTS

This work was funded by the Natural Sciences and Engineering Research Council of Canada [J.N.M., D.N., A.Z.], an Early Researcher Award from the Ministry of Research and Innovation [J.N.M.], the Human Frontier Science Program [Y.W.], and by the Arkansas Biosciences Institute, the major research component of the Arkansas Tobacco Settlement Proceeds Act of 2000 [Y.W.].

[1] V. C. Coffman and J.-Q. Wu, Trends in Biochemical Sciences **37**, 499 (2012).

[2] J. S. Verdaasdonk, J. Lawrimore, and K. Bloom, Methods in Cell Biology **123**, 347 (2014).

[3] M. B. Elowitz, A. J. Levine, E. D. Siggia, and P. S. Swain, Science (New York, N.Y.) **297**, 1183 (2002).

[4] A. Raj and A. van Oudenaarden, Cell **135**, 216 (2008).

[5] A. Eldar and M. B. Elowitz, Nature **467**, 167 (2010).

[6] D. Wang and S. Bodovitz, Trends in Biotechnology **28**, 281 (2010).

[7] C. Gawad, W. Koh, and S. R. Quake, Nature Reviews Genetics **17**, 175 (2016).

[8] G. Zhang, B. M. Ueberheide, S. Waldemarson, S. Myung, K. Molloy, J. Eriksson, B. T. Chait, T. A. Neubert, and D. Fenyo, Methods in Molecular Biology **673**, 211 (2010).

[9] V. C. Coffman and J.-Q. Wu, Molecular Biology of the Cell **25**, 1545 (2014).

[10] E. Betzig, G. H. Patterson, R. Sougrat, O. W. Lindwasser, S. Olenych, J. S. Bonifacino, M. W. Davidson, J. Lippincott-Schwartz, and H. F. Hess, Science (New York, N.Y.) **313**, 1642 (2006).

[11] M. Heilemann, S. van de Linde, M. Schüttpelz, R. Kasper, B. Seefeldt, A. Mukherjee, P. Tinnefeld, and M. Sauer, Angewandte Chemie **47**, 6172 (2008).

[12] S. van de Linde and M. Sauer, Chemical Society Reviews **43**, 1076 (2014).

[13] M. A. Thompson, M. D. Lew, and W. E. Moerner, Annual Review of Biophysics **41**, 321 (2012).

[14] P. Annibale, S. Vanni, M. Scarselli, U. Rothlisberger, and A. Radenovic, PloS ONE **6**, e22678 (2011).

[15] H. Deschout, A. Shivanandan, P. Annibale, M. Scarselli, and A. Radenovic, Histochemistry and Cell Biology **142**, 5 (2014).

[16] S.-H. Lee, J. Y. Shin, A. Lee, and C. Bustamante, Proceedings of the National Academy of Sciences **109**, 17436 (2012).

[17] A. Shivanandan, H. Deschout, M. Scarselli, and A. Radenovic, FEBS Letters **588**, 3595 (2014).

[18] N. Durisic, L. Laparra-Cuervo, A. Sandoval-Álvarez, J. S. Borbely, and M. Lakadamyali, Nature Methods **11**, 156 (2014).

[19] N. Durisic, L. L. Cuervo, and M. Lakadamyali, Current Opinion in Chemical Biology **20**, 22 (2014).

[20] C. R. Nayak and A. D. Rutenberg, Biophysical Journal **101**, 2284 (2011).

[21] G. C. Rollins, J. Y. Shin, C. Bustamante, and S. Pressé, Proceedings of the National Academy of Sciences of the United States of America **112**, E110 (2014).

[22] F. Fricke, J. Beaudouin, R. Eils, and M. Heilemann, Scientific Reports **5**, 14072 (2015).

[23] R. P. J. Nieuwenhuizen, M. Bates, A. Szymborska, K. A. Lidke, B. Rieger, and S. Stallinga, PloS ONE **10** (2015).

[24] R. Jungmann, M. S. Avendaño, M. Dai, J. B. Woehrstein, S. S. Agasti, Z. Feiger, A. Rodal, and P. Yin, Nature Methods **13**, 439 (2016).

[25] G. Hummer, F. Fricke, and M. Heilemann, Molecular Biology of the Cell , DOI:10.1091/mbc.E16 (2016).

[26] S. Tal and J. Paulsson, Plasmid **67**, 167 (2012).

[27] L. Wasserman, *All of Statistics A Concise Course in Statistical Inference* (Springer, 2009).

[28] Y. Wang, Y. Penkul, and J. N. Milstein, Biophysical Journal **11**, 467 (2016).

[29] "https://www.addgene.org/17655/,".

[30] M. A. Smith and M. J. Bidochka, Canadian Journal of Microbiology **44**, 351 (1998).

[31] R. Rocha, R. S. Santos, P. Madureira, C. Almeida, and N. F. Azevedo, Journal of Biotechnology **226**, 1 (2016).

[32] J. J. Schmied, A. Gietl, P. Holzmeister, C. Forthmann, C. Steinhauer, T. Dammeyer, and P. Tinnefeld, Nature Methods **9**, 1133 (2012).